ULUSLARARASI 3B YAZICI TEKNOLOJİLERİ
VE DİJİTAL ENDÜSTRİ DERGİSİ
INTERNATIONAL JOURNAL OF 3D PRINTING
TECHNOLOGIES AND DIGITAL INDUSTRY

ISSN:2602-3350 (Online)
URL: https://dergipark.org.tr/ij3dptdi

LASER POLISHING OF ADDITIVELY MANUFACTURED TITANIUM ALLOY IN OPEN AIR ATMOSPHERE

Yazarlar (Authors): Tolgahan ERMERGEN*, Fatih TAYLAN

Bu makaleye şu şekilde atıfta bulunabilirsiniz (To cite to this article): *Ermergen T., Taylan F., "Laser Polishing of Additively Manufactured Titanium Alloy in Open Air Atmosphere" Int. J. of 3D Printing Tech. Dig. Ind., 7(3): 456-470, (2023).*

DOI: 10.46519/ij3dptdi.1350367

Araştırma Makale/ Research Article

Erişim Linki: (To link to this article): https://dergipark.org.tr/en/pub/ij3dptdi/archive

LASER POLISHING OF ADDITIVELY MANUFACTURED TITANIUM ALLOY IN OPEN AIR ATMOSPHERE

Tolgahan ERMERGEN[a]*, Fatih TAYLAN[a]

[a]Isparta University of Applied Sciences, Faculty of Technology, Department of Mechanical Engineering, TURKEY

* *Corresponding Author:* tolgahanermergen@isparta.edu.tr

(**Received:** 26.08.23; **Revised:** 19.10.23; **Accepted:** 20.11.23)

ABSTRACT

Additive manufacturing has witnessed remarkable growth, transforming the production of intricate geometries. However, post-processing is often required to enhance surface quality and alleviate residual stresses in additively manufactured components. Laser polishing, an advanced technique, efficiently reduces surface roughness in metals. This study stands out by conducting laser polishing without protective gas in an open atmosphere. Results demonstrate that surface roughness can be improved by up to 50% under these conditions. Nevertheless, the process introduces a recast layer with significant oxidation due to atmospheric oxygen, leading to the formation of a Titanium Oxide layer and the development of surface microcracks. As oxidation increases, surface hardness also rises. Achieving high-quality surfaces for additively manufactured Ti alloys in an open atmosphere is attainable, provided vigilant monitoring of oxidation-related challenges. This study reveals the intricate relationship between laser polishing, surface characteristics, and the effects of open-air conditions on Ti-6Al-4V components.

Keywords: Laser Polishing, Surface Roughness, Ti-6Al-4V, Open Atmosphere Process.

1. INTRODUCTION

Additive Manufacturing (AM) techniques have brought about a transformative shift in the production of intricate metal parts, a task that poses significant challenges using traditional manufacturing approaches. Industries like aeronautics, medicine, and transportation have increasingly embraced AM due to its capacity to fabricate complex shapes and efficiently create customized components [1]. The strengths of AM encompass its aptitude for intricate designs, a diverse array of materials, and the ability to scale up personalized production [2-5]. While AM methods span a variety of materials for crafting intricate objects, metals [6-7], ceramics [8], polymers [9], and plastics [10] constitute some of the more prevalent choices. Among these, Fused Deposition Modelling (FDM) has emerged as a favored method for producing plastics and polymers [11-13]. In contrast, when it comes to metals and ceramics, Selective Laser Melting (SLM) has emerged as a prominent contender. SLM employs lasers to precisely melt and then fuse particles, thereby crafting successive layers during the fabrication process [14].

However, despite the myriad benefits of AM, certain drawbacks persist, notably concerning surface quality. The layer-by-layer construction inherent in AM can yield surfaces that fail to meet desired standards. This limitation stems from various AM-associated phenomena, including the "ladder effect" and "balling effect." The ladder effect is particularly pronounced on inclined or curved surfaces, introducing imperfections in surface quality. Conversely, the balling effect results in increased surface roughness due to variations in laser power, scanning speed, or powder diameter. This effect gives rise to undesirable ball-like structures on the surfaces of additively manufactured metal parts [15-16].

To surmount these limitations in surface quality, post-manufacturing treatments have become indispensable. Employing appropriate post-processing techniques can significantly enhance the surface quality of additively

manufactured components. By addressing these challenges head-on, AM methods can continue to evolve and find wider applications across diverse industries.

One favored approach for refining post-manufacturing surface quality is laser polishing (LP). This method involves a thermal-based process that employs lasers to refine surface characteristics. As outlined by Temmler et al. [2], laser polishing centers on the concept of re-melting and subsequently solidifying the surface using laser radiation, as depicted in Figure 1.

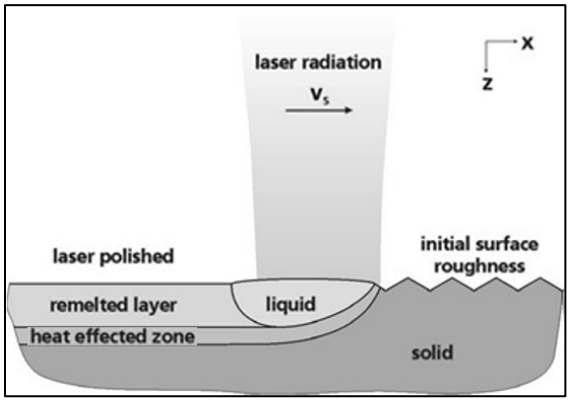

Figure 1. Schematics of the laser polishing process [2].

Laser polishing is employed to smooth out surface peaks on specimens by subjecting them to laser radiation that induces re-melting. When a laser beam with a sufficiently high energy density interacts with the material surface, surface peaks liquefy and flow toward lower-lying valleys due to the combined effects of gravity and surface tension. This process is illustrated in Figure 2 [4]. Following this, as the material cools down, the molten areas solidify, resulting in structurally sound regions devoid of pores. By mitigating the morphological inconsistencies on the surface, the overall surface quality is enhanced. This phenomenon was detailed in the research conducted by Temmler et al. [3].

Titanium stands out as a prominent material in AM processes owing to its favorable combination of high strength-to-weight ratio, corrosion resistance, and fracture toughness, as previously highlighted [17] and [18]. Given the substantial machining demands associated with conventionally manufactured Ti64 alloys to achieve the final form, Safavi et al. [19] have noted that additive manufacturing of Ti alloy components has gained considerable attention. This is because the near-net-shape production of additively manufactured Ti parts minimizes the need for extensive machining.

A plethora of studies on laser polishing of Titanium alloys are available in the literature, with a focus on reducing surface roughness values. However, many of these experiments were conducted within specific protective atmospheres such as Argon, Nitrogen, or CO_2. These controlled atmospheres prevent oxidation of the specimen surface during laser polishing. Notably, Ciganovic et al. [20] conducted surface modification on titanium implants using a TEA CO_2 laser under various gas atmospheres, including ambient air. The results indicated that polishing samples in an air atmosphere led to oxidation of the samples. For instance, the oxygen concentration before the operation was 4.3 wt.%, but it rose to approximately 36 wt.% after polishing. The polished materials exhibited varied surface colorization, ranging from white to deep purple, with sporadic yellow-gold hues.

Similarly, Ageev et al. [21] improved Ti surfaces using a laser under an open atmosphere, with the goal of generating oxide layers on the material surface. Their findings revealed the formation of a multilayered composite film on the surface. The lower layers consisted of Ti_2O_3 and TiO oxides along with titanium nitride, while the thin upper layer comprised transparent titanium dioxide. In an experiment, Perez del Pino et al. [22] observed the formation of both rutile and anatase TiO_2 layers on laser-polished Ti alloy, resulting in a flat and porous surface. Jaritngam et al. [23] investigated the enhancement of surface quality, recast thickness, and heat-affected zone depth of laser-polished Ti-6Al-4V components in ambient air. This process led to an average improvement of 43% in surface roughness. Additionally, the amount of oxygen within the polished surface correlated with the heat input; it decreased when a lower heat input was applied to the material surface.

Zeng et al. [24] have investigated the reactions between pure Ti and atmospheric air under laser surface modification operations. The study has shown that the phase transformation steps during the laser melting and subsequent cooling were found to be αTi→βTi→

αTi+βTi→αTi+TiN+TiNx→liquid+TiN→TiN +TiOxNy→TiO_2+TiN. Titanium nitrides appeared first, while TiO_2 was only observed during the cooling process, resulting from the solidification of the pre-existing liquid titanium oxides or the reaction between TiN and O_2.

It was also found that Oxygen was gathered mostly in the outermost surface layer, while Nitrogen mainly existed beneath the Oxygen rich layer.

The objective of this article is to investigate the surface characterization of the open-atmosphere laser polished of additively manufactured Ti-6Al-4V samples. Since laser polishing studies in the literature were conducted under controlled atmosphere, it is also aimed at questioning the possibility of the same process in a complete open-air atmosphere. In this study, the accuracy of the experiments and the core of the study have been supported by a DOE model and a SEM image comparison of the samples.

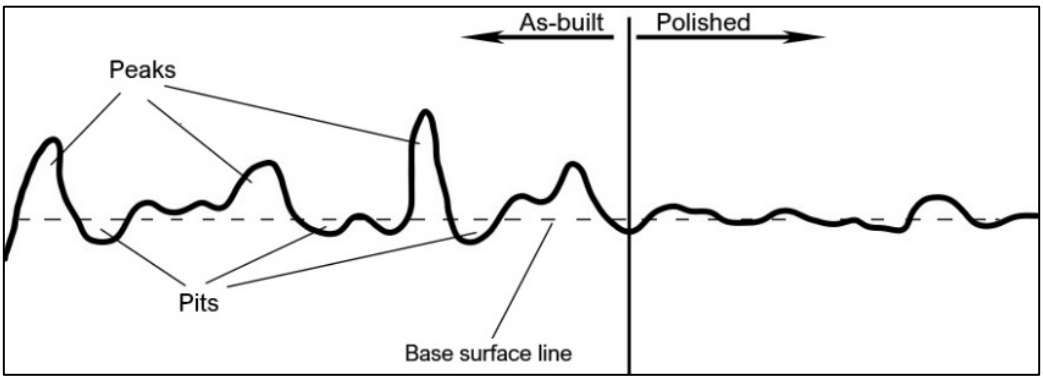

Figure 2. Principle of Laser Polishing [4]

2. MATERIAL AND METHOD

2.1. Additive Manufacturing Process

The AM system employed in this research was an EOSSint M280. This system falls under the category of SLM devices and is primarily utilized for creating intricate and complex geometries. Throughout the study, the manufacturing process utilized Ti-6Al-4V Grade 5 powder for fabricating the specimens.

The EOSSint M280 system is equipped with a heated build chamber, boasting dimensions of 250 mm x 250 mm x 325 mm. It relies on a continuous Ytterbium fiber laser with a wavelength of 1070 nm, and a maximum power capacity of 250 W. To preserve material integrity, the manufacturing process was meticulously carried out within an Argon atmosphere, preventing oxidation.

The manufacturing parameters adhered to default settings, as illustrated in Table 1, for consistent and reproducible production of the specimens.

Table 1. Printing Parameters used by EOSSint M280 SLM Device in the Study

Technical Specification	Value
Laser power	170 W
Beam wavelength	1070 nm
Scanning speed	1250 mm/s
Layer thickness	30 µm
Hatching distance	0.1 mm
Assist gas	Argon
Assist gas supply flow rate	100 l/min
Work mode	Continuous

2.2. Powder Used in The Study

The study utilized Ti alloy powder (EOS Ti64 9011-0014) supplied by the manufacturer, with a particle size ranging from 15 to 63 µm. The powder was generated through plasma atomization within a controlled environment of high-purity argon. This meticulous process ensured the production of particles with uniformly spherical surfaces, enhancing their character and quality. SEM image of EOS Ti64 9011-0014 powder was previously investigated by Lee et al. [25]. In the SEM image shown in Figure 3, particle shapes and the size distribution of the powders can be seen. The chemical composition of Ti64 Grade 5 powder, provided by the supplier [26], is shown in Table 2.

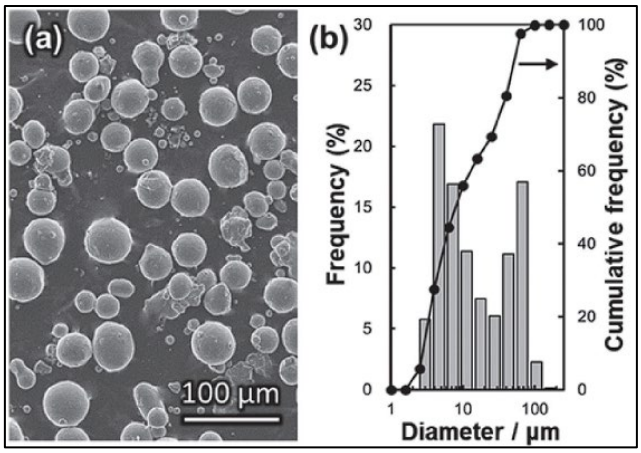

Figure 3. (a) SEM Images and (b) Particle Size Distribution of Ti-6Al-4V Grade 5 powder EOS Ti64 9011-0014 [25]

Table 2. Chemical Compositions of Ti64 Grade 5 (%wt)

Al	V	C	Fe	N	O	H	Ti
5.5 – 6.75	3.5 – 4.5	0.08	0.30	0.05	0.2	0.0125	Other

2.3. Sample Geometry

For this study, square-surface samples, as shown in Figure 4, with 12 mm x 12 mm surface dimensions and 0.91 mm thickness were chosen.

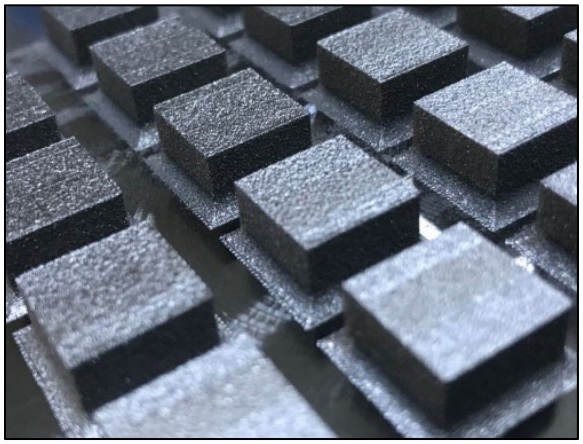

Figure 4. Ti64 Specimens Used in The Study

The purpose of the samples having a thickness of 0.91 mm is to try to form the final manufacturing layer with an angle of 90 degrees. Since the laser polishing process is aimed at being performed through the same angle, 0.91 mm thickness was the smallest dimension to be able to acquire.

2.4. Laser Polishing Process

The laser employed in this research to facilitate the laser polishing procedure was a Gaussian Type 20 W pulsed fiber laser. Operating at a frequency of 100 kHz and emitting at a wavelength of 1080 nm, this laser source played a pivotal role in the polishing process. Notably, the entire polishing procedure was carried out in an open-air environment. The specifics of the laser scan track, the laser scan offset utilized in the laser polishing process, and the ultimate orientation of the sample's final layer are visually depicted in Figure 5.

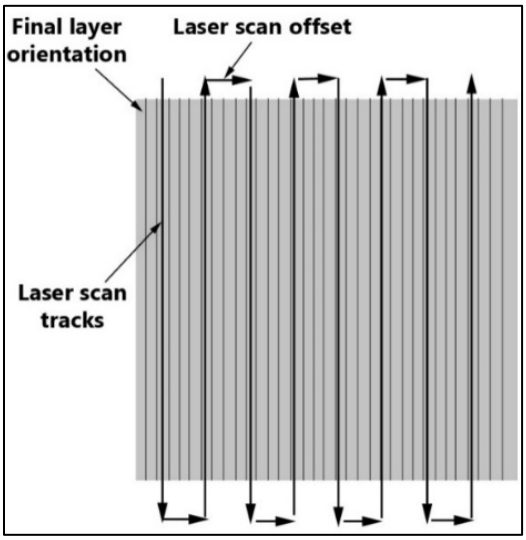

Figure 5. Scanning Strategy and Final Layer Orientation of the Samples

A preliminary polishing test was performed in order to investigate the most significant range for processing parameters affecting the resulting surface roughness. During preliminary tests, not only the parameters significantly affecting the surface quality, but also the parameters barely affecting the results were chosen for the parameter range for a sound

investigation. The range of processing parameters used in this study is given in Table 3. As seen, a total of 120 polishings were performed in this study.

Since laser polishing is a thermal-based process, the key principle for successful polishing is the adjustment of the energy density (ED) of the melt pool. Numerous energy density computation methods are present in the existing literature. In this investigation, the energy density (ED) calculation followed the formula proposed by Jaritngam et al. [23]. Equation 1 outlines the specific formula recommended for determining the energy density in pulsed laser treatment of titanium alloys.

$$ED = \frac{N_{so}\ x\ P}{V\ x\ d}\ (\mathrm{J/cm^2}) \quad (1)$$

In this context, the symbols represent the following parameters: P denotes laser power (W), d stands for the diameter of the laser beam (mm), V represents scanning speed (mm/s), and N_{So} signifies the count of reheating events. The occurrence of N_{So} transpires during the polishing process owing to scan overlap, and its quantification is articulated in Equation 2.

$$N_{so} = ceil\ (\frac{100}{100-\%S_o}) \quad (2)$$

where $\%S_o$ refers the percentage of scan overlap, which is given in Eq 3 below;

$$\%S_o = 100\ x\ \frac{d-s}{d} \quad (3)$$

where d is the diameter of the laser beam (mm) and s is the stepover distance (mm).

Table 3. Process Parameter Range Used in The Study

Laser Power (W)	Scanning Speed (mm/s)	Beam Overlap (%)
3-6-9-12-15-18	75-100-125-150-175	0-30-60-90

3. EXPERIMENTAL FINDINGS AND RESULTS

3.1. Final Surface Quality (R_a) Values

Involving 120 specimens, this study employed diverse process parameters, as outlined in Table 3. Experimental results yielded s R_a% improvement ranging from 1.48% to 50.27%. The highest improvement, 50.37%, occurred at 2571 J/cm² energy density, utilizing 18 W laser power, 175 mm/s scanning speed, and 90% beam overlap. Conversely, the lowest improvement, 1.48%, was noted at 86 J/cm² energy density, 6 W laser power, 175 mm/s scanning speed, and 0% beam overlap.

3.2. Influence of ED and Process Parameters

Unlike many prior studies that identify an optimal energy density (ED) range for optimal outcomes with particular materials, this study does not reveal a definitive ED range for superior results. While a potential optimal range appears roughly between 2000-3000 J/cm², graphically displaying the results indicates a lack of a clear-cut optimal ED range. Refer to Figure 6 shows the distribution of R_a% improvement across different ED values.

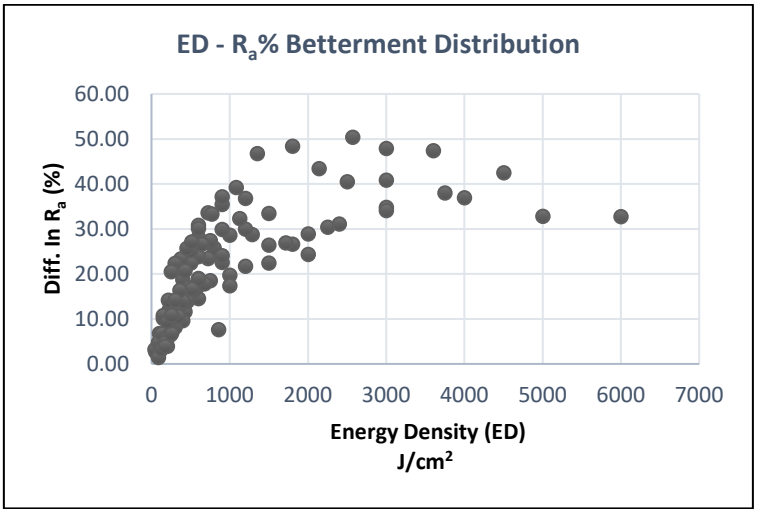

Figure 6. R_a% Betterment Distribution for Each ED in The Study

Take the case of an energy density (ED) of approximately 2000 J/cm² as an example. At this ED level, the potential improvement ratios range from 24.32% to 43.46%. It's evident that relying solely on ED values is not merely enough to assess outcomes. In conjunction with ED values, the corresponding parameters leading to that specific ED value – namely, laser power (P), scanning speed (V), and Beam Overlap – should also be taken into account.

A complete factorial design of experiments (DOE) model was employed to statistically analyze the impact of input process parameters on the ultimate outcome. The DOE model underscored the notable influence of laser power and beam overlap on output values, whereas scanning speed exhibited minimal effect. To put it succinctly, laser power and beam overlap emerge as primary determinants for anticipating final surface roughness. Meanwhile, scanning speed, although less influential on results, can be seen as a compensating factor within Equation 1 to achieve desired energy density (ED) values. The findings of the DOE model are summarized in Table 4.

Table 4. Input Parameter Influence of DOE Model

Resource	Sum of Squares	Average Square	F Values	P Values	Influence Rate (%)
Model	234.10	19.51	129.09	<0.0001	93.54
Laser Power	138.68	27.74	183.53	<0.0001	55.41
Scanning Speed	13.38	3.35	22.14	<0.0001	5.34
Beam Overlap	82.04	27.35	180.95	<0.0001	32.78
Error	16.17	0.1511			6.46
Total	250.27				100

S	R-sq	R-sq (adj)	R-sq (pred)
3.887	93.54%	92.81%	91.87%

The accuracy of this DOE model, which has been indicated as R-sq in Table 4, was calculated as 93.54%. In the same table, the influence rates of laser power, scanning speed, and beam overlap can also be seen. Laser power has a 55.41% influence rate, beam overlap has a 32.78% influence rate and scanning speed has only a 5.34% influence rate, as explained before.

In Figure 7, the effect of average values of parameters considered during laser polishing on average R_a% Betterment rates is given in graphs.

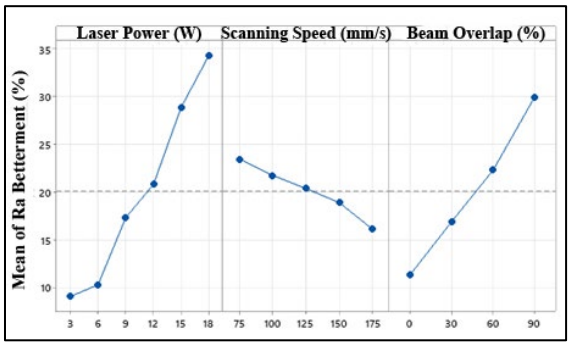

Figure 7. Effect of Average Values of Parameters During Laser Polishing on Average R_a% Betterment Rates

Figure 7 demonstrates that increasing the laser power and beam overlap leads to improved surface quality. This observation is further supported by the detailed graphs in Figure 8 and Figure 9, which also show similar results. Conversely, it appears that higher scanning speeds have a negative effect on the final outcome. However, upon analyzing the values provided in Table 4 and the detailed graph in Figure 10, it becomes evident that the change in scanning speed has a relatively minor impact on the final results.

When comparing these findings with similar studies in the literature, it is apparent that scanning speed is considered a significant parameter affecting the final outcome. Nonetheless, in this particular study, the influence of scanning speed on the output values was found to be insufficient. This discrepancy can be attributed to the different experimental conditions, as previous studies were conducted in a controlled atmosphere with significantly higher laser powers compared to those used in this research. Hence, the results obtained in this study are not in contradiction with the existing literature.

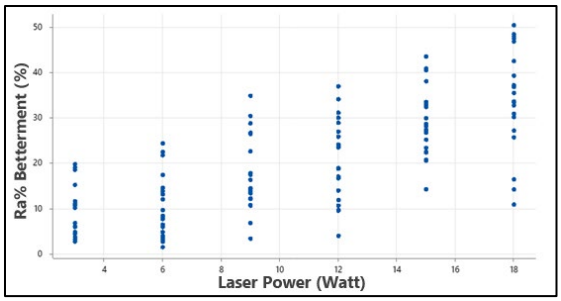

Figure 8. Effect of Laser Power on R_a% Betterment Rate

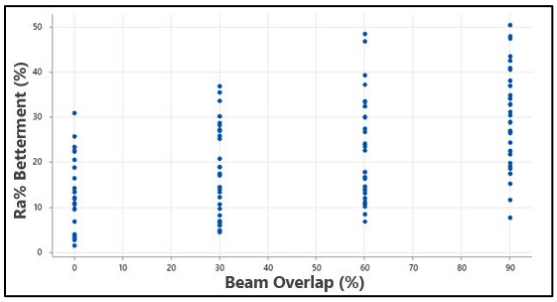

Figure 9. Effect of Beam Overlap on R_a% Betterment Rate

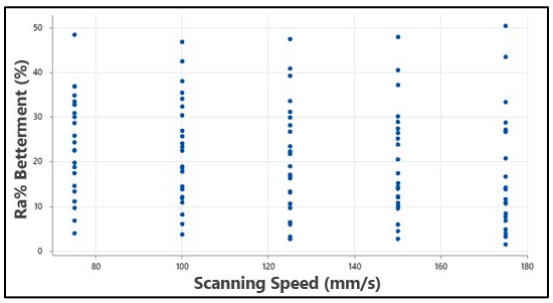

Figure 10. Effect of Scanning Speed on R_a% Betterment Rate

3.3. SEM Analyzes

The surface changes of the samples at different magnifications were examined in the SEM photographs taken with the electron microscope. Figure 11 shows the SEM image at 100x magnification of the as-built sample, which was not subjected to laser polishing.

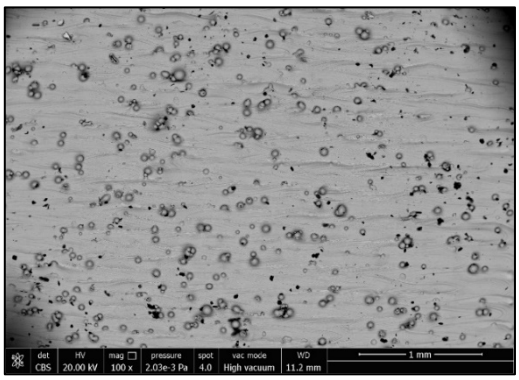

Figure 11. SEM Image of The As-built Sample at 100x Magnification

When Figure 11 is examined, it is seen that there are too many unmelted powder particles on the surface of the as-built sample. In this phenomenon called balling, powder particles form powder lumps on the surface as they cannot be fully melted and sintered to each other. As a result of this balling effect, the surface quality of the material is adversely affected. When the larger scale SEM images in Figures 12 and 13 are examined, the details of the balling effect and the existence of waving on the surface can be clearly seen.

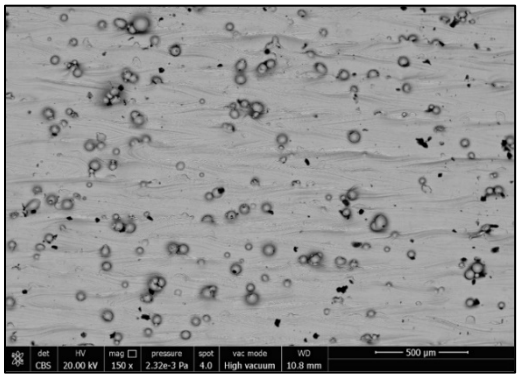

Figure 12. SEM Image of The As-built Sample at 150x Magnification

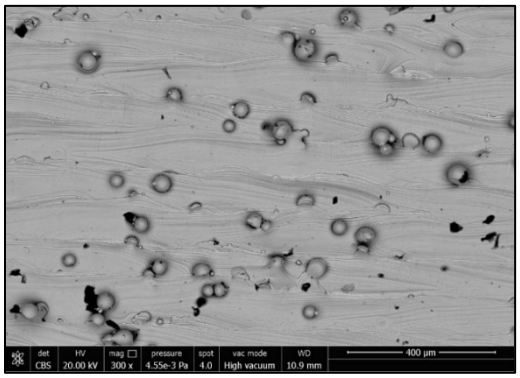

Figure 13. SEM Image of The As-built Sample at 300x Magnification

When the SEM images of experiment 37, which had the lowest result with a betterment rate of 1.48%, were examined, images similar to those obtained in the as-built sample were acquired. In Figure 14, the SEM image of sample 37 at 100x magnification is compared with the SEM image of the as-built sample at the same magnification. It is seen that with a betterment of 1.48%, the balling effect and waving can be clearly displayed on the surface of sample 37, which has almost the same surface quality as the as-built sample. It is observed that there is no change in the surface structure of sample 37 processed with 6 W laser power, 175 mm/s

scanning speed, 0% beam overlap ratio, and an energy density of 86 J/cm^2. Considering the 150x and 300x magnification SEM images given in Figures 15 and 16, it is proven that there is no change in the surface structure of sample 37.

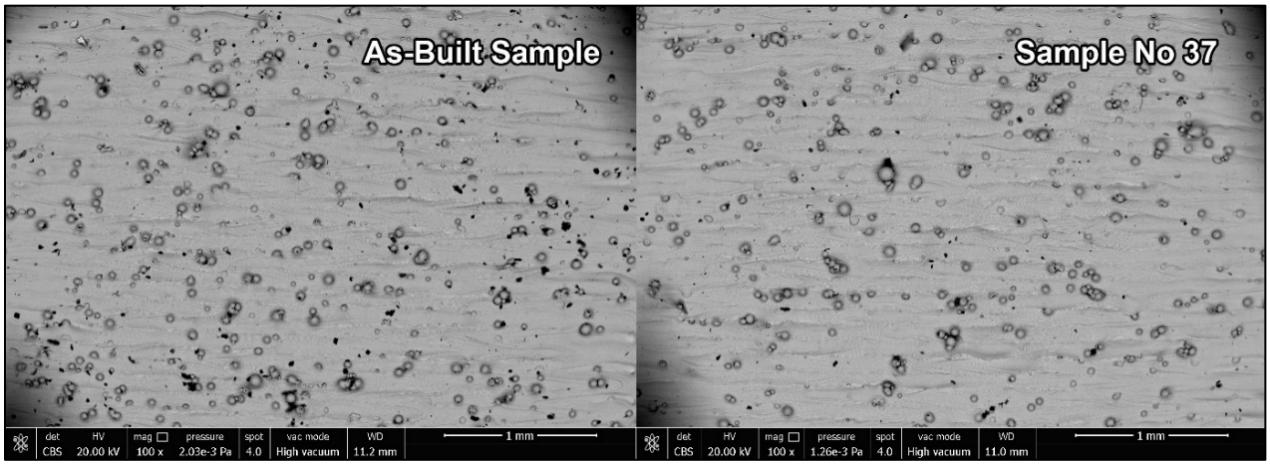

Figure 14. SEM Images Comparison of As-Built Sample and Sample No. 37 at 100x Magnification

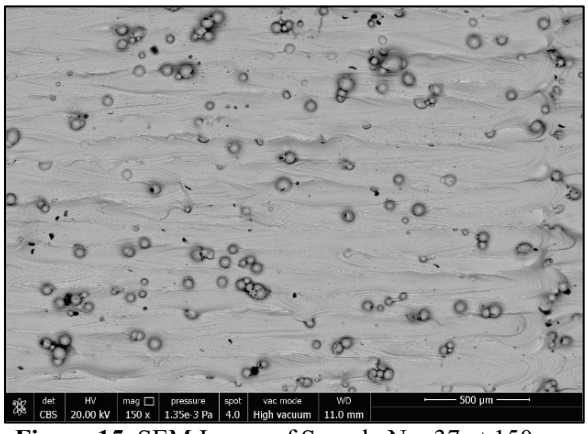

Figure 15. SEM Image of Sample No. 37 at 150x Magnification

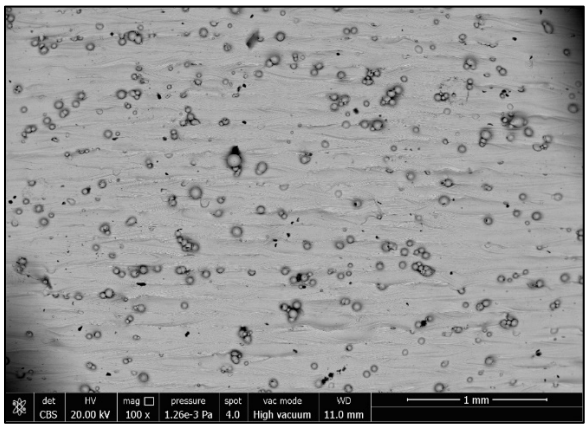

Figure 16. SEM Image of Sample No. 37 at 300x Magnification

When the SEM images of experiment no. 120, which achieved the best result with a betterment rate of 50.37%, are examined, the effect of the surface quality increment can be clearly observed. In the SEM image with 100x magnification given in Figure 17, it is seen that the balling effect on the sample surface 120 is almost eliminated and the wavy surface structure is improved.

The micrograph in Figure 17d shows a comparison between the polished and as-built regions of sample No. 120. In the as-built region on the left side of the image, the presence of unmelted powder particles is clearly visible, whereas in the polished region on the right side of the image, these unmelted powder particles are absent, and a smoother surface is observed. In the 100x magnification SEM image in Figure 17a, it is evident that the surface of sample No. 120 is significantly smoother compared to the raw sample.

When examining the SEM image of sample No. 120 at 1,000x magnification in Figure 17e, it can be observed that microcracks have formed during the laser polishing process. During laser polishing carried out in an open atmosphere, the Ti element on the surface reacts with oxygen to form Titanium Oxide layers such as TiO, TiO_2, or Ti_2O_3. These layers have mismatched surface tensions with the underlying Ti-6Al-4V layers, resulting in the formation of microcracks on the surface [26]. Additionally, the heating and cooling cycles during laser polishing cause a solid-phase $\beta \rightarrow \alpha$ transformation in titanium, leading to the visibility of grain boundaries, contributing to the observed image. Although

the image in Figure 17e may appear to show major cracks, the visibility of grain boundaries should not be interpreted as cracks [27, 28].

Surface tension mismatch leads to the formation of microcracks on the specimen surface, which adversely affects fatigue resistance. Moreover, these microcracks can propagate under any stress on the surface. In a study conducted on train rails by Beretta et al. [29], it was noted that microcracks resulting from different surface tensions progressed toward the interior layers of the material, ultimately negatively impacting the component's fatigue strength.

To prevent crack formation, laser polishing should be performed in an atmosphere-protected environment [30]. Given that the laser polishing process within the scope of the study was performed in an open atmosphere, it is important to consider that there was no controlled atmosphere process. Therefore, it is not possible to completely eliminate crack formation. However, measures such as preheating the workpiece may slow down the crack formation process.

Crack formation occurs due to the oxidation on the material surface resulting in the formation of Titanium Oxide layers [26]. As known, Titanium Oxides are considered as ceramics. Hence, after the laser polishing process, two different material types are present in the sample: Titanium Oxides in the ceramic class and the Ti-6Al-4V alloy in the metal class. The mechanical and thermal properties of these materials are provided in Table 5 [31, 32, 33].

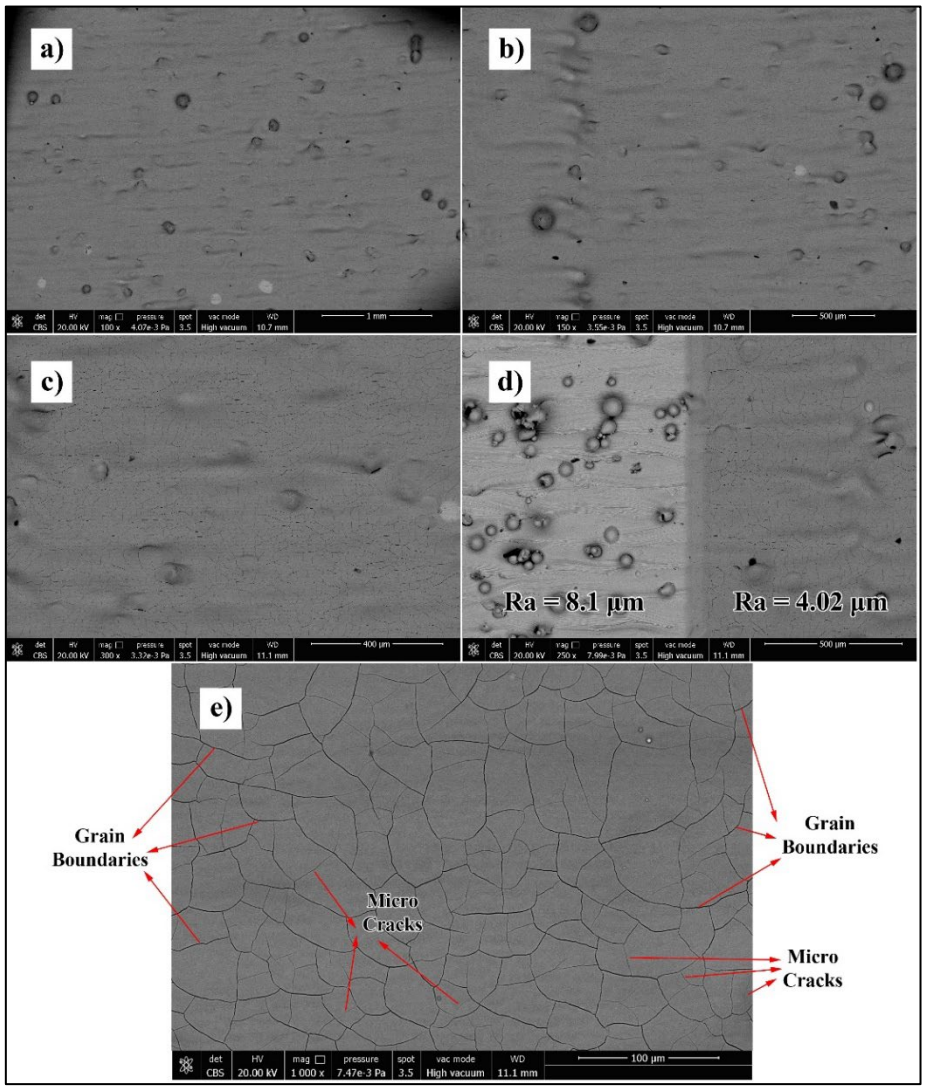

Figure 17. SEM Image of Sample No.120, a) at 100x Magnification, b) at 150x Magnification, c) at 300x Magnification, d) comparison of as-built and polished surfaces, e) at 1000x Magnification

Table 5. Mechanical and Thermal Properties of Ti-6Al-4V and TiO_2 [31, 32,33]

	Ti-6Al-4V	TiO_2
Young Modulus (GPa)	110-119	230-288
Hardness (HV)	343-360	951-1049
Coefficient of Thermal Expansion (10-6/K)	8.7-9.1	8.4-11.8

When examining Table 5, it is evident that TiO_2 is more brittle, and its coefficient of thermal expansion is more variable. Therefore, due to the abrupt thermal changes occurring on the sample surface during the laser polishing process, the responses of the Titanium Oxide layers on the sample surface and the Ti-6Al-4V alloy immediately beneath these layers to thermal changes will be different. The surface tensions between these two materials trigger the formation of microcracks on the sample surface [27]. Although crack formation cannot be entirely prevented [28], the quantity of microcracks and, consequently, their adverse effects on fatigue resistance can be reduced. In this context, preheating the workpiece with a heating table during the laser polishing process can reduce the amount of abrupt temperature change on the sample, damping the impact of microcracks that may occur due to thermal shock. Additionally, due to their different coefficients of thermal expansion and Young's Modulus values, potential delamination between the Titanium Oxide layer and the Ti-6Al-4V layer, resulting from both thermal and mechanical loads, can be prevented.

3.4. EDS Analyzes

EDS analyses were also performed with the same device on the samples that were analyzed by electron microscopy. In this step, elemental analysis and chemical characterization are carried out as a result of the interaction of the X-ray with the sample, so the weight percent distribution of the elements in the sample can be determined.

Before the elemental analysis of the samples that did not undergo LP treatment, the as-built sample was subjected to elemental EDS analysis under a scanning electron microscope. In the graph given in Figure 18, the elemental analysis of the as-built sample as a percentage by weight is given. According to this analysis, the as-built sample contains 84.65% Titanium, 4.24% Vanadium, 5.98% Aluminum and 5.12% Oxygen. These values are given in detail in Table 6.

When these values are examined with the chemical content of EOS Ti64 9011-0014 powder given in Table 2, it is seen that the amount of Oxygen in the samples increased slightly as a result of the manufacturing and subsequent separation from the table by the wire erosion method.

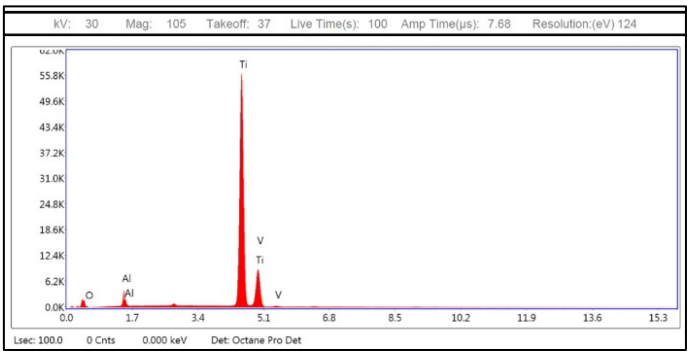

Figure 18. EDS Analysis Graph of As-Built Sample

Table 6. EDS Analysis Result of As-Built Sample

Element	Wt %	Atomic %	Net Int.	% Error
O	5.12	13.39	16.10	14.09
Al	5.98	9.26	277.24	8.19
Ti	84.65	73.87	6654.91	0.98
V	4.24	3.48	277.48	2.68

When sample 37, which has almost no difference in surface quality with a recovery rate of 1.48%, was examined, results similar to the data obtained in the raw sample were obtained.

The EDS analysis chart in Figure 19 and the analysis results in Table 7 are given in the sample No.37, containing 83.48% Titanium, 4.36% Vanadium, 5.55% Aluminum and 6.62% Oxygen. In this case, it can be said that there is no significant change in the chemical characterization of sample 37 treated with an ED of 86 J/cm^2.

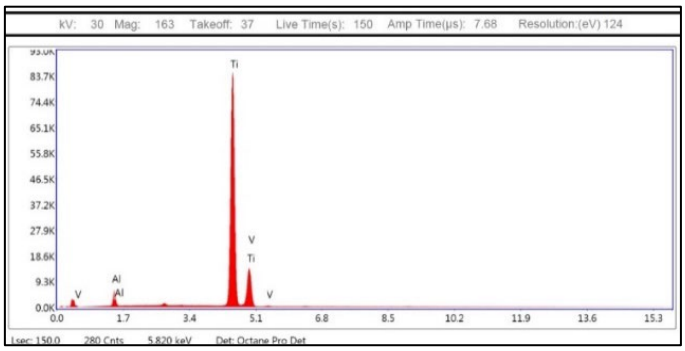

Figure 19. EDS Analysis Graph of As- Sample No.37

Table 7. EDS Analysis Result of Sample No.37

Element	Wt %	Atomic %	Net Int.	% Error
O	6.62	19.90	24.44	12.79
Al	5.55	8.40	261.67	8.10
Ti	83.48	71.21	6693.45	0.94
V	4.36	3.50	290.94	2.33

When sample No.120, which achieved the highest result with a recovery rate of 50.37%, is examined, it is seen that the results differ significantly. When the EDS analysis of sample No.120 processed with an ED of 2571 J/cm^2 is performed, it is seen that the amount of Oxygen contained in the sample has increased to 20.74%.

The EDS analysis graph in Figure 20 and the analysis results in Table 8 in sample No.120 were determined to absorb more Oxygen by entering into a chemical reaction with the Oxygen in the atmosphere as a result of the heat generated on the surface. In this regard, it can be deduced that sample No.120 has a higher oxide layer compared to the as-built sample or sample No.37.

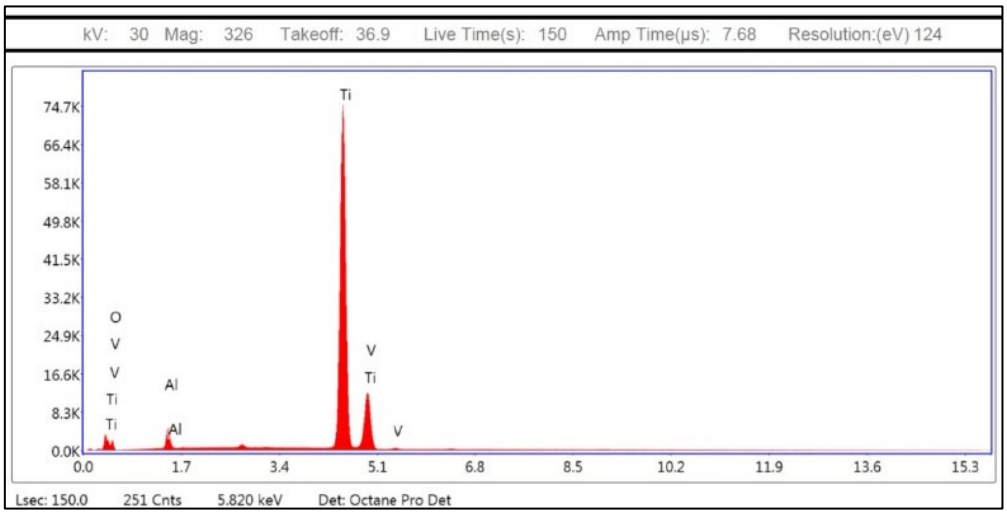

Figure 20. EDS Analysis Graph of As- Sample No.120

Table 8. EDS Analysis Result of Sample No.120

Element	Wt %	Atomic %	Net Int.	% Error
O	20.74	42.95	79.56	11.03
Al	4.49	5.51	220.07	8.04
Ti	70.91	49.04	5845.78	0.91
V	3.86	2.51	265.62	2.27

In the study, the graph in Figure 21 was drawn with the results obtained as a result of the EDS analysis of the laser polished samples. This graph shows the relationship between the $\%R_a$ betterment rate and the amount of Oxygen contained in the samples.

As can be seen from the graph, similar Oxygen amounts were observed at certain $\%R_a$ betterment rate ranges. In this regard, the Oxygen content of the samples with a surface quality improvement rate of up to 15% is close to the as-built sample, while the Oxygen content increases to 10%-17% at 15%-30% betterment ratios, and to 20%-22% Oxygen content at 15%-30% betterment ratios. Although it is understood that the rate of surface quality improvement has an effect on the amount of Oxygen contained, it can be seen that the relationship between these parameters is not very sensitive.

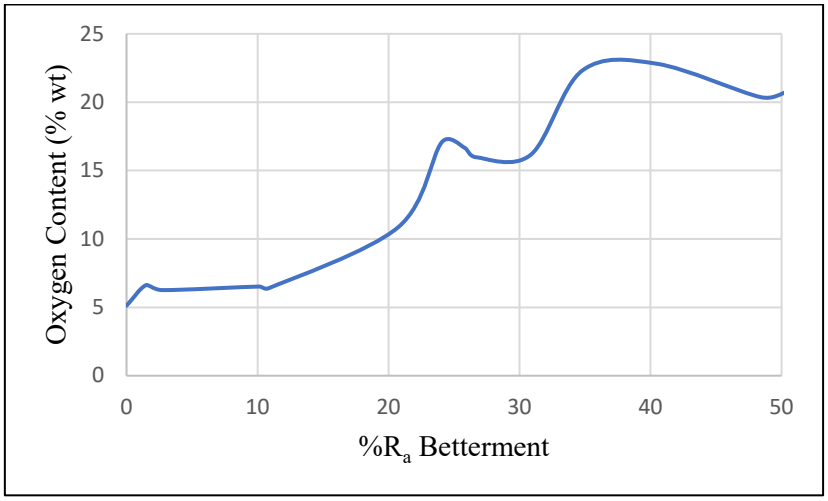

Figure 21. The relationship between $\%R_a$ betterment rate and the amount of Oxygen contained

3.5. Surface Hardness Measurement

As a result of EDS analysis, it was determined that the amount of Oxygen on the surface increased, thus forming oxide structures in the chemical compound of the sample. The effect of these oxidations on the surface on the hardness of the sample was tested by microhardness measurement.

As a result of the microhardness measurement on the Vickers scale, where a preload of 1 kg was applied for 15 seconds, the hardness value of the as-built sample was measured at 462.8 HV. It was 478.9 HV for sample No.37 with the least improvement in surface quality, and 651.1 HV for sample No.120

When the hardness value of sample No.37 is examined, it is seen that there is no significant difference between it and the as-built sample. As a matter of fact, considering the amount of Oxygen they contain, there was no significant difference between the as-built sample and sample No.37. For this reason, it is expected that the hardness value of the sample No.37 is very close to the as-built sample. On the other hand, the hardness increase in sample No.120, which contains 20.74% Oxygen by weight in its chemical structure, was 40.68% and became 651.1 HV.

In Figure 22, the graph describes the relationship between the Oxygen content and the surface hardness values of 120 samples for which hardness measurements were made

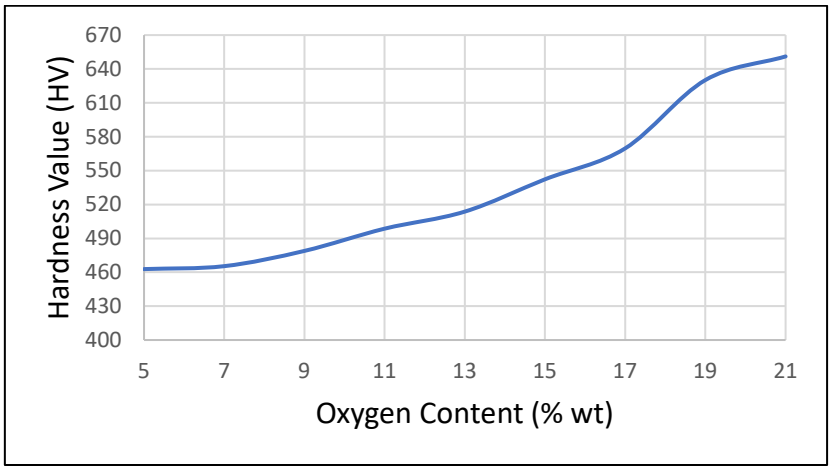

Figure 22. The relationship between the hardness value and the amount of Oxygen contained

4. CONCLUSION

In this study, additively manufactured Ti-6Al-4V samples were subjected to laser polishing in a complete open-air atmosphere to investigate the possibility of this operation along with its consequences. The results obtained at the end of this experiment were listed below.

- Even though the majority of the laser polishing processes in the literature were performed in a controlled atmosphere, a laser polishing operation in a completely open atmosphere is possible. However, a vigilant monitoring should be required for the potential adverse effects of the oxidation.
- At the end of the experiment, a surface betterment ratio of 50,37% can be achieved.
- During the experiment, it is seen that the energy density itself is not enough to evaluate the output of the experiment. Along with energy density, the parameters used in the experiment, which are laser power, scanning speed, and beam overlap ratio, also play an important role on the output.
- Despite the surface quality enhancement, microcracks on the surface structure occurred. This situation was the result of Titanium Oxide formation.
- The hardness of the sample surfaces increases by increasing the Oxygen content during the LP.

REFERENCES

1. Grimm, T., Wiora, G., Witt, G., "Characterization of Typical Surface Effects In Additive Manufacturing With Confocal Microscopy", Surface Topography: Metrology and Properties, Vol. 3 Issue 1, 2015.

2. Temmler, A., Willenborg, E., Wissenbach, K., "Design surfaces by laser remelting", Physics Procedia, Vol. 12, Issue A, Pages 419–430, 2011.

3. Temmler A., Willenborg E., Wissenbach K., "Laser Polishing", In Laser Applications in Microelectronic and Optoelectronic Manufacturing (LAMOM) XVII 2012, Proceedings of Vol. 8243, San Francisco, California, United States, 2012.

4. Ermergen T., Taylan F., "Review on Surface Quality Improvement of Additively Manufactured Metals by Laser Polishing", Arabian Journal for Science and Engineering, Vol. 46, Pages 7125-7141, 2021.

5. Perez M., Carou D., Rubio E.M., Teti R., "Current advances in additive manufacturing" Procedia CIRP, Vol. 88, Pages 439-444, 2020.

6. Ermergen T., Taylan F., "Investigation of DOE model analyses for open atmosphere laser polishing of additively manufactured Ti-6Al-4V samples by using ANOVA" Optics & Laser Technology, Vol. 168, 2024.

7. Gardner L., "Metal additive manufacturing in structural engineering – review, advances, opportunities and Outlook", Structures, Vol. 47, Pages 2178-2193, 2023.

8. Wu D., Yu X., Zhao Z., Ma G., Zhou C., Zhang B., Ren G., Niu F., "One-step additive manufacturing of TiCp reinforced Al2O3–ZrO2 eutectic ceramics composites by laser directed

energy deposition", Ceramics International, Vol. 49, Issue 8, Pages 12758-12771, 2023.

9. Ergene B., Bolat Ç., "An experimental study on the role of manufacturing parameters on the dry sliding wear performance of additively manufactured PETG", The Journal of International Polymer Processing, Vol. 37, Issue 3, Pages 255-270, 2022.

10. Mishra V., Negi S., Kar S., "FDM-based additive manufacturing of recycled thermoplastics and associated composites", Journal of Material Cycles and Waste Management, Vol. 25, Pages 758-784, 2023.

11. Ergene B., Yalçın B., "Eriyik yığma modelleme (EYM) ile üretilen çeşitli hücresel yapıların mekanik performanslarının incelenmesi", Gazi Üniversitesi Mühendislik Mimarlık Fakültesi Dergisi, Vol. 38, Issue 1, Pages 201-218, 2023.

12. Patel R., Desai C., Kushwah S., Mangrola M.H., "A review article on FDM process parameters in 3D printing for composite materials", Materials Today: Proceedings, Vol. 60, Issue 3, Pages 2162-2166, 2022.

13. Marşavina L., Valean C., Marghitaş M., Linul E., Razavi N., Berto F., Brighenti R., "Effect of the manufacturing parameters on the tensile and fracture properties of FDM 3D-printed PLA specimens", Engineering Fracture Mechanics, Vol. 274, 2022.

14. Sefene M.E., "State-of-the-art of selective laser melting process: A comprehensive review", Journal of Manufacturing Systems, Vol. 63, Pages 250-274, 2022.

15. Brooks H., Rennie A., Abram T., "Variable fused deposition modelling— analysis of benefits, concept design and tool path generation", In: Innovative Developments in Virtual and Physical Prototyping, Pages 511–517, 2011.

16. Gu, D., Shen, Y., "Balling phenomena in direct laser sintering of stainless-steel powder: metallurgical mechanisms and control methods", Materials & Design, Vol. 30, Issue 8, Pages 2903–2910, 2009.

17. Zhang L-C., Attar H., "Selective Laser Melting of Titanium Alloys and Titanium Matrix Composites for Biomedical Applications: A Review", Advanced Engineering Materials, Vol. 18, Issue 4, Pages 463-475, 2015.

18. Saboori A., Gallo D., Biamino S., Fino P., Lombardi M., "An Overview of Additive Manufacturing of Titanium Components by Directed Energy Deposition: Microstructure and Mechanical Properties", Applied Sciences, Vol. 17, Issue 9, Pages 883, 2017.

19. Safavi M.S., Bordbar-Khiabani A., Khalil-Allafi J., Mozafari M., Visai L, "Additive Manufacturing: An Opportunity for the Fabrication of Near-Net-Shape NiTi Implants", Journal of Manufacturing and Materials Processing, Vol. 6, Issue 3, Page 65, 2022.

20. Ciganovic J., Stasic J., Gakovic B., Momcilovic M., Milovanovic D., Bokorov M., Trtica M., "Surface modification of the titanium implant using TEA CO2 laser pulses in controllable gas atmospheres – Comparative study", Applied Surface Science, Vol. 258, Pages 2741-2748, 2012.

21. Ageev E.I., Andreeva Y.M., Karlagina Y.Y., Kolobov Y.R., Manokhin S.S., Odintsova G.V., Slobodov A.A., Veiko V.P., "Composition analysis of oxide films formed on titanium surface under pulsed laser action by method of chemical thermodynamics", Laser Physics, Vol. 24, Issue 7, 2017.

22. Perez del Pino A., Serra P., Morenza J.L., "Laser Surface Processing of Titanium in Air: Influence Of Scan Traces Overlapping", Journal of Laser Applications, Vol. 15, Issue 120, 2003.

23. Jaritngam P., Tangwarodomnukun V., Qi H., Dumkun C., "Surface and Subsurface Characteristics of Laser Polished Ti6Al4V Titanium Alloy", Optics&Laser Technology, Vol. 126, 2020.

24. Zeng C., Wen H., Zhang B., Sprunger P.T., Guo S.M., "Diffusion of Oxygen and Nitrogen into Titanium under Laser Irradiation in Air", Applied Surface Science, Vol. 505, Issue 1, 2019.

25. Lee S., Oh J.Y., Mukaeyama S., Sun S., Nakao T., "Preparation of Titanium Alloy/Bioactive Glass Composite for Biomedical Applications via Selective Laser Melting", Material Transactions, Vol. 6, Issue 9, Pages 1779-1784, 2019.

26. Li P., Wang Y., Li L., Gong Y., Zhou J., "Ablation oxidation and surface quality during laser polishing of TA15 aviation titanium alloy", Journal of Materials Research and Technology, Vol.23, Pages 6101-6114, 2023

27. Tian, Y., Gora, W.S., Cabo, A.P., Parimi, L. L., Hand, D.P., Tammas-Williams, S., Prangnell, P.B., "Material interactions in laser polishing powder bed additive manufactured Ti6Al4V components", Additive Manufacturing, Vol. 20, Pages 11-22, 2018.

28. Lee, S., Ahmadi, Z., Pegues, J., W., Mahjouri-Samani, M., Shamsaei, N., "Laser polishing for

improving fatigue performance of additive manufactured Ti-6Al-4V parts", Optics & Laser Technology, Vol. 134, 2021.

29. Beretta S., Ghidini A., Lombardo F., "Fracture mechanics and scale effects in the fatigue of railway axles", Engineering Fracture Mechanics, Vol. 72, Issue 2, Pages 195-208, 2005

30. Bhaduri D., Penchev P., Batal A., Dimov S., Soo S.L., Sten S., Harrysoon U., Zhang Z., Dong H., "Laser polishing of 3D printed mesoscale components", Applied Surface Science, Vol. 405, Pages 29-46, 2021.

31. Kasperovich G., Hausmann J., "Improvement of fatigue resistance and ductility of TiAl6V4 processed by selective laser melting," Journal of Materials Processing Technology, Vol. 220, Pages 202-214, 2015.

32. Shunmugavel, M., Polishettu A., Nomani J., Goldberg M., Littlefair G., "Metallurgical and Machinability Characteristics of Wrought and Selective Laser Melted Ti-6Al-4V", Journal of Metallurgy, Vol. 2016, 2016.

33. AZO Materials Home Page. https://www.azom.com/properties.aspx?ArticleID=1547. Access Date, 2023-03-02.